Polymer 50 (2009) 1965–1974

Contents lists available at ScienceDirect

Polymer

journal homepage: www.elsevier.com/locate/polymer

A comprehensive study of the interactions between DNA and poly(3,4-ethylenedioxythiophene)

Carlos Alemán [a,*], Bruno Teixeira-Dias [a], David Zanuy [a], Francesc Estrany [b], Elaine Armelin [a], Luis J. del Valle [c,*]

[a] Departament d'Enginyeria Química, ETSEIB, Universitat Politècnica de Catalunya, Av. Diagonal 647, 08028 Barcelona, Spain
[b] Unitat de Química Industrial, EUETIB, Universitat Politècnica de Catalunya, Comte d'Urgell 187, 08036 Barcelona, Spain
[c] Departament d'Enginyeria Agroalimentària i Biotecnología, ESAB, Universitat Politècnica de Catalunya, Av. Canal Olímpic 15, 08860 Castelldefels, Spain

ARTICLE INFO

Article history:
Received 18 November 2008
Received in revised form
17 February 2009
Accepted 20 February 2009
Available online 28 February 2009

Keywords:
Polythiophene
DNA
Conducting polymer

ABSTRACT

The interaction between poly(3,4-ethylenedioxythiophene), a conducting polymer with excellent electrical and electrochemical properties, and plasmid DNA has been investigated using electrophoresis, UV–visible and CD spectroscopy, and quantum mechanical calculations. Analyses of mixtures with different DNA:polymer mass ratios indicate that, in all cases, interactions form immediately and induce structural alterations in DNA. Furthermore, the existence of interactions between poly(3,4-ethylenedioxythiophene) and specific nucleotides sequences has been evidenced by adding restriction enzymes to the mixtures. In contrast, interactions between DNA and poly(3-methylthiophene), a similar polyheterocyclic conducting polymer but without hydrogen bonding acceptors, are weak or do not exist. These results suggest that, in addition to non-specific electrostatic interactions between the charged phosphate groups of DNA and the positively charged fragments of the conducing polymers, specific hydrogen bonding interactions play a crucial role. The ability of 3,4-ethylenedioxythiophene units to form hydrogen bonds with the methylated analogues of DNA bases has been examined in different environments using MP2/6-31G(d) and MP2/6-311++G(d,p) calculations. Results indicate that, in environments with low polarity, the formed interactions are significantly stronger than those reached by unsubstituted thiophene and similar to those established by pyrrole. However, in polar environments (aqueous solution) 3,4-ethylenedioxythiophene provides stronger interactions with nucleic acids than both thiophene and pyrrole. These theoretical results are fully consistent with experimental observations.

1. Introduction

The interaction of conducting electroactive polymers, such as polythiophene (PTh), polypyrrole (PPy) and their derivatives, with selected bioentities (*e.g.* amino acids [1–3], proteins [2–7], DNA and oligonucleotides [8–18], and living cells [19–23]) is a subject of increasing interest [24,25]. The quest to interact more efficiently with biosystems, to obtain information related to system performance and to control that performance remain not only an exciting but also an essential area of research. Thus, the development of biotechnological applications based on conducting polymers greatly depends on the control of such interactions.

Within this area of research we are particularly interested in the interaction of conducting polymers with DNA sequences, which may have great implications in numerous medical applications ranging from diagnosis to gene therapy [8–18,24,25]. The interaction of p-doped electroactive materials with DNA has been traditionally attributed to the tendency of the latter to interact with positively charged molecules. However, in recent studies we found that some conducting polymers, for example PPy, are able to interact forming specific interactions with well-defined nucleotide sequences of plasmid DNA [15–17]. This selectivity suggests that polymer:DNA adducts are stabilized not only by electrostatic interactions but also by interactions that act specifically, *i.e.* interactions that depend on the chemical environment, the spatial disposition and orientation of the chemical groups, etc. In particular, the importance of specific hydrogen bonding interactions in these complexes is expected to be significantly greater than those that are non-specific, *e.g.* stacking, van der Waals and charge transfer interactions. Indeed, we found that all the conducting polymers able to form specific interactions with DNA contain functional groups that are excellent donors and acceptors of hydrogen bonds [15–17], *e.g.* the N–H in PPy or the ester side groups

* Corresponding authors.
E-mail addresses: carlos.aleman@upc.edu (C. Alemán), luis.javier.del.valle@upc.edu (L.J. del Valle).

0032-3861/$ – see front matter © 2009 Elsevier Ltd. All rights reserved.
doi:10.1016/j.polymer.2009.02.033

in some PTh derivatives. Furthermore, we recently used sophisticated theoretical calculations to show that hydrogen bonding interactions between DNA bases and PPy are significantly stronger than interactions between DNA bases and PTh, the later lacking of hydrogen bonding donors and acceptors [18].

Within a recent study devoted to examine the potential applications of different materials [15,16], we preliminary investigated the interaction between DNA and two different PTh derivatives using qualitative electrophoretic assays. Specifically, the conducting polymers examined were poly(3,4-ethylenedioxythiophene), in which dioxane rings are fused onto thiophene rings, and poly(3-methylthiophene), hereafter denoted PEDOT and PT3M, respectively. Interestingly, we found that PEDOT interacts specifically with plasmid DNA forming strong and stable complexes. This feature together with its remarkable electrochemical stability and electrical properties [26–29], and notable electro-biocompatibility [22,23] make this material a good candidate for different biotechnological applications that involve DNA, *e.g.* biosensor and drug-delivery system. In contrast, PT3M, a PTh derivative without hydrogen bonding donors and acceptors, only formed stable adducts at very high DNA:polymer mass ratios, and specific interactions were significantly weaker than in DNA:PEDOT. Attracted by this field, in this work we report a comprehensive study about the microscopic details of the interactions between plasmid DNA and PEDOT using both experimental and computational methods.

Specifically, the interaction of PEDOT with plasmid DNA has been examined considering different DNA:polymer mass ratios and using electrophoresis, UV–visible spectroscopy and circular dichroism (CD). The possible formation of specific interactions has been examined by the digestion of DNA:PEDOT mixtures using restriction enzymes, which cut off at specific nucleotide sequences. Furthermore, ab initio quantum mechanical calculations have been used to examine the strength of the specific interactions between PEDOT and DNA. Calculations have been performed considering the building blocks of the two interacting systems, *i.e.* 3,4-ethylenedioxythiophene (EDOT) units and methylated analogues of DNA bases [9-methyladenine (mA), 1-methylthymine (mT), 1-methylcytosine (mC) and 9-methylguanine (mG)], as well as environments with different polarity.

2. Methods

2.1. Synthesis and characterization

3,4-Ethylenedioxythiophene (EDOT), 3-methylthiophene (T3M) and acetonitrile of analytical reagent grade were purchased from Aldrich and used as-received. Anhydrous lithium perchlorate, analytical reagent grade, from Aldrich was stored in an oven at 80 °C before its use in the electrochemical trials.

PEDOT and PT3M films were generated by anodic polymerization using a VersaStat II potentiostat–galvanostat connected to a computer controlled through a Power Suite Princenton Applied Research program. Electrochemical experiments were conducted in a three-electrode two-compartment cell under nitrogen atmosphere (99.995% in purity) at 298 K. The working compartment was filled with 40 ml of a 10 mM monomer solution in acetonitrile containing 0.1 M $LiClO_4$ as supporting electrolyte. A volume of 10 ml of the same electrolyte solution was placed in the cathodic compartment. Steel AISI 316 sheets of 4 cm^2 area were employed as working and counter electrodes. The reference electrode was an Ag|AgCl electrode containing a KCl saturated aqueous solution ($E0 = 0.222$ V at 25 °C), which was connected to the working compartment through a salt bridge containing the electrolyte solution. Electrogeneration of PEDOT and PT3M was carried out by CA under a constant potential of 1.40 and 1.70 V, respectively, a polymerization time $\theta = 900$ s being used in both cases. Uniform, adherent and insoluble polymeric films were obtained by this procedure, the coloration being dark-blue and black for PEDOT and PT3M, respectively. The electrical and electrochemical characterizations of the materials derived from these experimental conditions was previously reported [15,26].

Ultrafine particles of polymer were used to interact with DNA. These were obtained by applying ultrasounds to a polymer solution (5 μg polymer/μl; milliQ water), which was prepared by considering the polymer samples grinded with a mortar. The dimensions of the resulting particles were analyzed using scanning electron microscopy (SEM) with a JSM-6400 JEOL microscope.

2.2. Formation of DNA:PEDOT complexes and electrophoretic assays

DNA:PEDOT complexes were prepared upon aqueous solutions by mixing 4 μl of plasmid pMT4 (0.05 μg/μl) with 0.00, 0.05, 0.50, 2.50 and 5.00 μl of polymer solution (5 μg polymer/μl; milliQ water), which corresponded to the desired DNA:PEDOT mass ratios (1:0, 1:1, 1:10, 1:50, 1:100, respectively). Final volumes were raised to 13 μl with sterile milliQ water. The mixtures were incubated overnight at 37 °C. After this, an aliquot of 6× gel loading buffer was added, samples being centrifuged for 10 min. The supernatant was analyzed by electrophoresis with 1% of agarose gel containing ethidium bromide (0.5 μg/ml of gel) in 1× tris–acetate–EDTA buffer (TAE). To evaluate the cleavage of pMT4 with EcoRI and BamHI in DNA:PEDOT complexes, 1 μl of restriction enzyme (10 000 U/ml) and 1.56 μl of 10× enzyme buffer was added to each incubated sample. The digestion process was carried out at 37 °C for 1 h, the digested products being analysed by electrophoresis.

2.3. Spectroscopic studies

A Nicolet Evolution 300 (Thermo Electron Co.) spectrophotometer controlled by the Vision Pro software was used to record UV–visible spectra of DNA:PEDOT and DNA:PT3M complexes at 22 °C, in the 200–1000 nm range, with a bandwidth of 2 mm and a scan speed of 600 nm/min. Light scattering effects were avoided by correcting the maximum absorbance of nucleotide bases in DNA, which is 260 nm (A_{260nm}), with respect to the absorbance at 350 nm (A_{350nm}). For each sample, 36 cycles separated by an interval of 5 min between consecutive cycles were recorded.

CD measurements were carried out in a Jasco J-810 spectropolarimeter at 22 °C using a quartz cuvette. The CD data were recorded with standard sensitivity (100 mdeg), in the 170–360 nm range, with bandwidth of 2 mm, response time of 0.5 s and scanning speed of 500 nm/min. The reported spectra correspond to the average of five scans, the raw spectra being smoothed by the Savitsky–Golay algorithm and deconvolutioned for analysis and interpretation. For each sample, the CD spectrum of the polymer was subtracted from that of the DNA:polymer complex, and compared with the CD spectrum of the plasmid DNA.

2.4. Quantum mechanical calculations

Calculations were performed using the Gaussian 03 [30] computer program. The structures of the complexes were determined by full geometry optimization in the gas-phase at the MP2 level [31] with the 6-31G(d) basis set [32], frequency calculations being performed to obtain the zero-point vibrational energies and both the thermal and entropic corrections. Single point energy calculations were performed on the MP2/6-31G(d) geometries at the MP2/6-311++G(d,p) [33] level. In order to estimate the free energies in the gas-phase, the statistical corrections obtained at the

MP2/6-31G(d) level were added to the electronic energies computed at the MP2/6-311++G(d,p) level.

The counterpoise (CP) method was applied to correct the basis set superposition error [34]. The binding energies, which were obtained with and without apply the CP ($\Delta E_{b,g}^{CP}$ and $\Delta E_{b,g}$ respectively), were calculated at the MP2/6-311++G(d,p) level as the difference between the total energy of the optimized complex and the energies of the isolated monomers with the geometries obtained from the optimization of the complex.

The effect of the solvent on the relative stability of the complexes was estimated using the polarizable continuum model (PMC) developed by Miertus, Scrocco and Tomasi [35,36]. This SCRF method involves the generation of a solvent cavity from spheres centered at each atom in the molecule and the calculation of virtual point charges on the cavity surface representing the polarization of the solvent. The magnitude of these charges is proportional to the derivative of the solute electrostatic potential at each point calculated from the molecular wavefunction. Then, the point charges are included in the one-electron Hamiltonian inducing polarization of the solute. An iterative calculation is carried out until the wavefunction and the surface charges are self-consistent.

PCM calculations were performed in the framework of the ab initio MP2 level with the 6-31G(d) basis set and using the standard protocol and considering the dielectric constants of chloroform ($\varepsilon = 4.9$) and water ($\varepsilon = 78.4$). Calculations were performed considering the gas-phase optimized geometries. Thus, solvent-induced changes in bond lengths and angles have been proved to have small influence on the free energy of solvation (ΔG_{sol}) [37–39], *i.e.* solute geometry relaxations in solution and single point calculations on the gas-phase optimized geometries provide almost identical values of ΔG_{sol}. The relative free energies and the binding energies in solution, which provide information about the relative stability of the complexes and the strength of the interactions in solution, respectively, were computed using the classical thermodynamics schemes.

3. Results and discussion

PEDOT films were prepared by chronoamperometry (CA) under a constant potential of 1.4 V. The electrogenerated films were grinded mechanically using a mortar. Scanning electron micrographs of the resulting samples (Fig. 1a) showed that they are constituted by plates of large dimensions, *i.e.* larger than 50 μm, which preclude their use for the present study. In order to reduce the size of the PEDOT particles, ultrasounds were applied to a solution prepared with such grinded samples. This process led to ultrafine particles with dimensions ranging between 3 and 18 μm (Fig. 1b) that are suitable to interact with biological macromolecules.

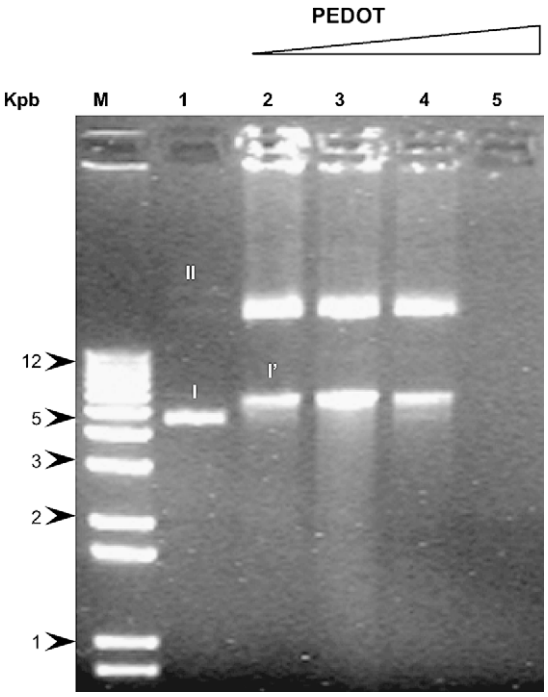

Fig. 2. Interaction of pMT4 plasmid DNA and increasing concentrations of PEDOT after their incubation for 3 h at 37 °C. Lane M: molecular weight marker (1 Kb Plus DNA Ladder). Lane 1: pMT4 plasmid DNA (1:0 DNA:PEDOT). Lanes 2–5: 1:1, 1:10, 1:50 and 1:100 DNA:PEDOT mass ratios. Labels I and II indicate form I and II of pMT4 plasmid DNA, respectively. Label I' refers to mobility alterations in the form I of plasmid DNA.

The formation of DNA:PEDOT complexes was evidenced by electrophoresis (Fig. 2), different DNA:polymer mass ratios (1:1, 1:10, 1:50 and 1:100) being considered for analyses. Lane 1 corresponds to the pMT4 plasmid (1:0 ratio), and shows a mixture of the supercoiled form I (bottom or band at the front) and the singly nicked form II (top or band at the back). Lanes 2–5, which display the DNA:PEDOT series at 1:1, 1:10, 1:50 and 1:100 ratios, reflect significant alterations in the bands associated to pMT4 evidencing the formation of complexes. Specifically, DNA:polymer complexes retard the mobility of form I and increase the intensity of form II. The variation in the mobility undergone by the former band is probably due to the conformational changes induced by the conducting polymer in the plasmid DNA during the formation of the corresponding DNA:PEDOT complexes. Accordingly, hereafter form I' will refer to the altered form I. As can be seen, DNA:PEDOT

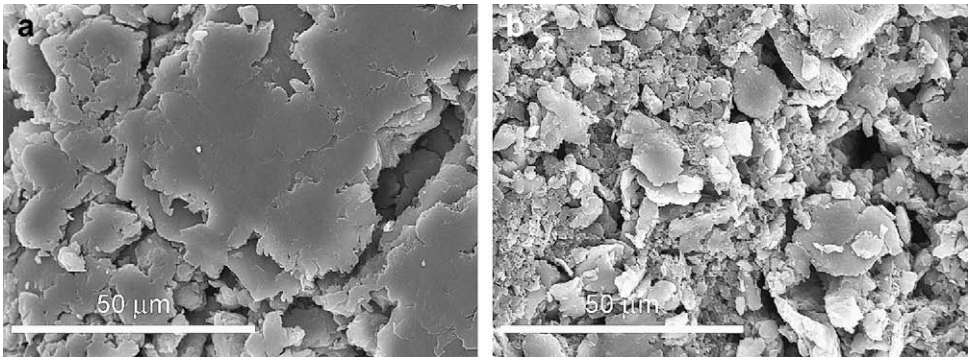

Fig. 1. Scanning electron micrographs of PEDOT particles obtained by grinding the electrogenerated films (a) and by submitting to ultrasounds the grinded samples (b).

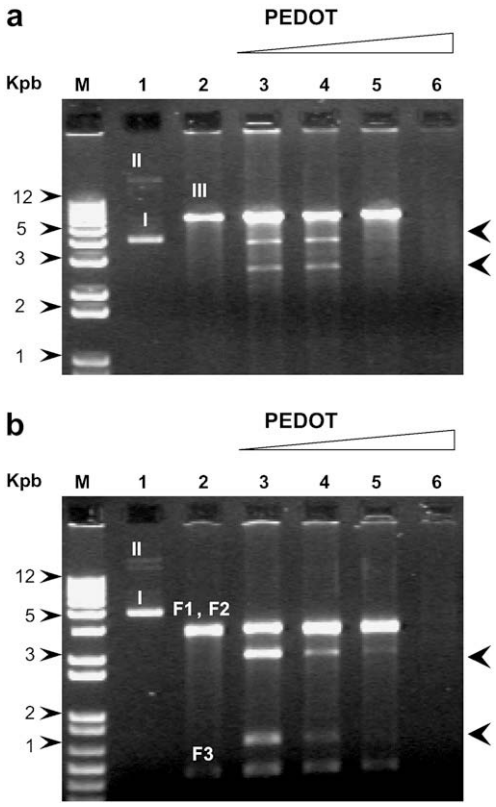

Fig. 3. Interaction between pMT4 plasmid DNA and increasing concentrations of PEDOT followed by EcoRI (a) and BamHI (b) enzymatic digestion for a period of 1 h at 37 °C. Lane M: molecular weight marker (1 Kb Plus DNA Ladder). Lane 1: undigested and untreated pMT4 plasmid DNA (1:0 ratio). Lane 2: digested pMT4 plasmid DNA (1:0 ratio). Lanes 3–6: 1:1, 1:10, 1:50, 1:100 DNA:PEDOT ratios after enzymatic digestion. Labels I–III refer to forms I, II and III of pMT4 plasmid DNA, respectively. F1–F3 indicates the DNA fragments obtained by digestion with BamHI. The head arrow indicates new topoisomers formed during the interaction between DNA and polymers.

complexes are formed for the four considered ratios. Specifically, interactions start at the 1:1 ratio, whereas all DNA is involved in the formation of stable adducts at the 1:100 ratio. Thus, the absence of bands in lane 5 must be attributed to the sedimentation of these adducts during the centrifugation process previous to the electrophoretic assay.

In order to look for specific interactions between the conducting polymer and the plasmid DNA, restriction enzymes were added to the incubated samples. These enzymes were EcoRI and BamHI, which cut off at 5′-G/AATTC-3′ and 5′-G/GATCC-3′ nucleotide sequences, respectively. The pMT4 plasmid DNA contains only one restriction site for EcoRI converting supercoiled form I and singly nicked circular form II into linear DNA (form III). BamHI has three restriction sites producing three DNA fragments, denoted F1, F2 and F3. The molecular weights of F1 and F2 are similar, their mobility in agarose gel corresponding to a single band. Fragment F3 presents the lowest molecular weight and, therefore, shows the fastest mobility. However, BamHI produces form III when it makes only one cut in the plasmid DNA.

The electrophoretograms obtained for DNA:PEDOT complexes after digestion with EcoRI and BamHI are displayed in Fig. 3. For each enzyme, lane 1 shows the untreated and undigested pMT4 plasmid DNA, lane 2 displays the digested plasmid DNA (1:0 DNA:PEDOT ratio), and lanes 3–6 correspond to the digested DNA:PEDOT complexes with increasing mass ratios. Digestion with EcoRI produces the band associated to the formation of linear DNA (form III) for 1:1, 1:10 and 1:50 ratios. However, as was found in the Fig. 2, the formation and subsequent sedimentation of DNA:PEDOT adducts preclude the detection of bands for the 1:100 ratio. The interaction of DNA with PEDOT at the 1:1 and 1:10 ratios promotes, after digestion with EcoRI, the formation of new topoisomers with higher mobility than linear DNA. Regarding the action of BamHI on DNA:PEDOT complexes (Fig. 3b), results are very similar to those described for EcoRI. Thus, the bands associated to F1–F3 are detected in lanes 3–5, whereas lane 6 reflects the formation of DNA:polymer adducts.

In order to provide details about the temporal evolution of the interaction between plasmid DNA and PEDOT, the behaviour of the nucleotide bases was investigated during the formation of the complexes by UV–visible spectrophotometry. Fig. 4 represents the evolution of $(A - A_0)/A_{max}$ against the time (t) for the 1:1 and 1:100 DNA:PEDOT mixtures, where A_0 corresponds to the absorbance of DNA in solution (1:0 DNA:PEDOT ratio) at the initial time ($t = 0$ min), A_{max} is the absorbance of the bases in the DNA:polymer mixture after thermal denaturalization of DNA *i.e.* the sample is heated at 94 °C during 15 min producing exposition of all DNA bases, and A is the absorbance of nitrogen bases in the DNA:PEDOT mixture measured at different times (cycles).

As can be seen, UV–visible results depend on the DNA:PEDOT mass ratio. The interaction between DNA and PEDOT is relatively low for the 1:1 ratio, which is reflected by the moderate exposition of the DNA nitrogen bases. In contrast, the degree of interaction found for the mixture with 1:100 mass ratio is very high. These strong interactions, which are formed immediately as revealed the fast exposition of the DNA nitrogen bases, are consistent with the formation of adducts previously evidenced by the electrophoretic assays.

For the sake of comparison, UV–visible spectra were also recorded for DNA:PT3M mixtures with 1:1 and 1:100 mass ratios

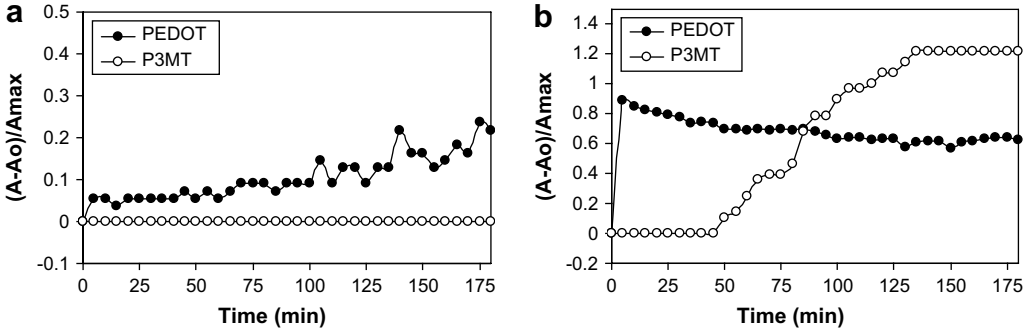

Fig. 4. Temporal evolution of DNA:PEDOT (-●-) and DNA:PT3M (-○-) mixtures with (a) 1:1 and (b) 1:100 DNA:polymer mass ratios followed by UV–visible spectroscopy (see text). Spectra were recorded during the 36 cycles, two consecutive cycles being separated by a 5 min interval.

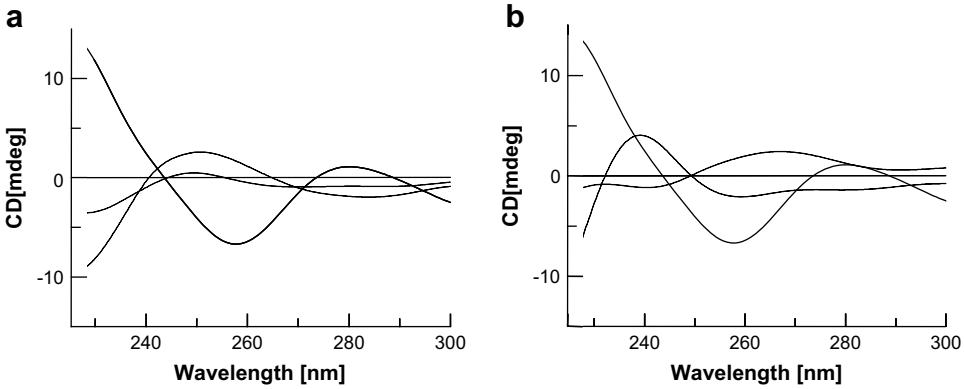

Fig. 5. CD spectra of DNA:polymer complexes to study the structural alterations of DNA: (a) DNA:PEDOT and (b) DNA:PT3M mixtures with 1:1 (——) and 1:100 (···) mass ratios. In all cases the CD spectrum of the corresponding conducting polymer was subtracted from the CD spectra of the DNA:polymer mixtures. The spectrum recorded for the pMT4 plasmid DNA (—) is also included.

(Fig. 4). Ultrafine particles of this conducting polymer were prepared by applying ultrasounds to grinded samples, which were electrogenerated by CA under a constant potential of 1.7 V. The exposition of the nitrogen bases reveals the absence of interactions between the plasmid DNA and the conducting polymer for the 1:1 ratio. Similarly, no interaction is detected during the first 50 min for the 1:100 ratio. After this, the exposition of the nitrogen bases increases slowly showing the formation of very stable DNA:PT3M adducts after 130 min. These results are fully consistent with the electrophoretograms previously reported for DNA:PT3M mixtures [15], which indicated that interactions between pWL102 plasmid DNA and PT3M are weak. In addition, digestion with EcoRI and BamHI showed that the protection imparted by PT3M to DNA is very small evidencing that specific interactions are weak or do not exist.

Structural alterations undergone by plasmid DNA when it interacts with PEDOT were examined by circular dichroism (CD) spectroscopic measurements. Fig. 5 compares the CD spectra recorded for plasmid DNA (1:0 ratio) and both DNA:PEDOT and DNA:PT3M mixtures with 1:1 and 1:100 ratios. In order to detect structural changes in DNA, the CD spectrum of the polymer (0:1 ratio) was subtracted from those of the mixtures.

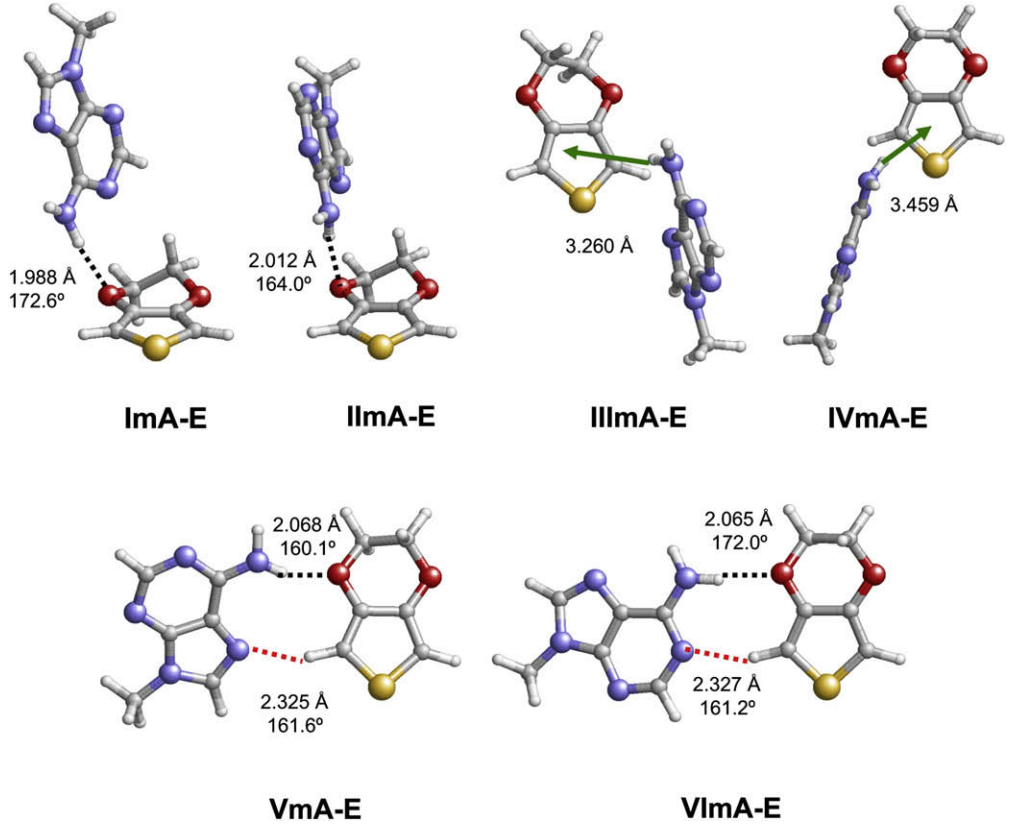

Fig. 6. Geometries of the six EDOT····mA minimum energy complexes calculated at the MP2/6-31G(d) level. N–H···O, C–H···O and N–H···π interactions are indicated by black dashed lines, red dashed lines and green arrows, respectively. Hydrogen bonding parameters (distances and angles) are displayed. (For interpretation of the references to color in this figure legend, the reader is referred to the web version of this article.)

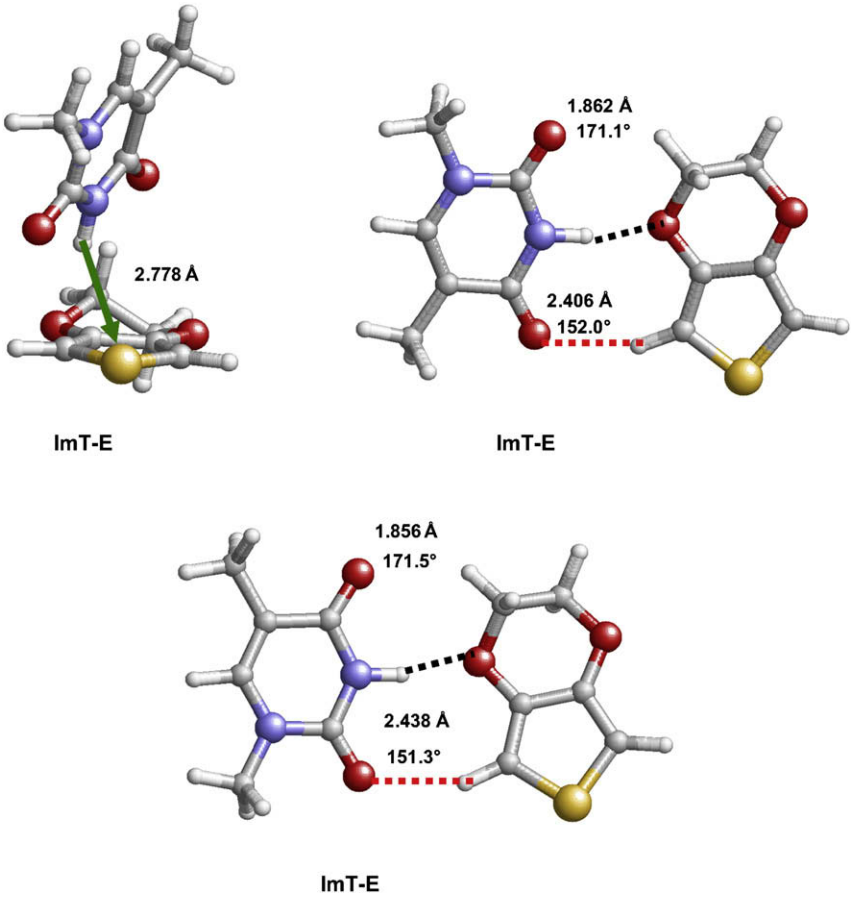

Fig. 7. Geometries of the three EDOT···mT minimum energy complexes calculated at the MP2/6-31G(d) level. N–H···O, C–H···O and N–H···π interactions are indicated by black dashed lines, red dashed lines and green arrows, respectively. Hydrogen bonding parameters (distances and angles) are displayed. (For interpretation of the references to color in this figure legend, the reader is referred to the web version of this article.)

The plasmid used in this work is a supercoiling circular DNA and its ellipiticity is negative. The raw CD spectra recorded between 200 and 360 nm show ellipiticity changes and loss of structure for the 1:100 DNA:PT3M mixture (Fig. 5b), while the two DNA:PEDOT mixtures maintain negative ellipticity but with loss of the supercoiling structure (Fig. 5a). On the other hand, DNA adopts the B-form in aqueous solution, the characteristics of the CD spectrum typically found for the canonical structure being the following: positive band at 275 nm, negative band at 245 nm and crossover point near 258 nm [40,41]. Fig. 5 indicates that the characteristic features of the pMT4 plasmid correspond to the B-form, even although small differences are detected with respect to the canonical form: positive band at 280 nm, negative signal at 257 nm, and crossover point near 270 nm. The appearance of the spectrum changes in the presence of the conducing polymers. The observed differences, which include a significant reduction in the intensity of the negative and positive bands, correspond to conformational variations. Unfortunately, the DNA structure in DNA:polymer mixtures cannot be clearly defined due to the presence of the light scattering of spectral tails. Thus, the size of the complexes can contribute for the light scattering [41].

The CD results conclude that the contact between plasmid DNA and PEDOT produces changes in the secondary structure of DNA. The immediate consequence of this structural alteration is the exposition of the DNA bases, which favors the rapid formation of interactions with PEDOT. Some of such interactions are with specific nucleotide sequences, like those found for the 5′-G/AATTC-3′ (target for EcoRI) and 5′-G/GATCC-3′ (target for BamHI) sequences, inducing the protective effect in the restriction cleavage. The formation of specific interactions involves not only directional preferences but also dependence on the chemical nature of the conducting polymer. These features are typically associated to hydrogen bonds. Thus, the importance of hydrogen bonds in DNA:polymer complexes with specific interactions is expected to be significantly greater than those that are of non-specific, *e.g.* stacking, van der Waals, electrostatic and charge transfer.

In order to ascertain the ability of EDOT units to form specific interactions with methylated nucleic acids (mNA), quantum mechanical calculations at the MP2[12] level were performed on EDOT···mNA complexes (where mNA = mA, mG, mC and mT). The EDOT unit was considered in the neutral (reduced) state rather than in the doped (oxidized) one. This is because in oxidized poly-conjugated polymers, as PEDOT and PTh, charges are not uniformly distributed along the whole molecular chains but are localized in small segments that involve a few number of repeating units (typically a few tenths of rings present a quinoid-like electronic structure) [42–46]. These segments are separated among them by blocks of rings with a benzenoid-like electronic structure, which is characteristic of conjugated heterocyclic species in the neutral state [42–46]. Neutral EDOT units belonging to non-charged blocks are expected to participate in the formation of specific hydrogen bonding interactions with DNA bases, while charged units are probably involved in non-specific electrostatic interactions with the phosphate groups of DNA.

A total of 26 starting geometries were prepared for EDOT···mNA complexes applying the following scheme: (i) the thiophene (Th)

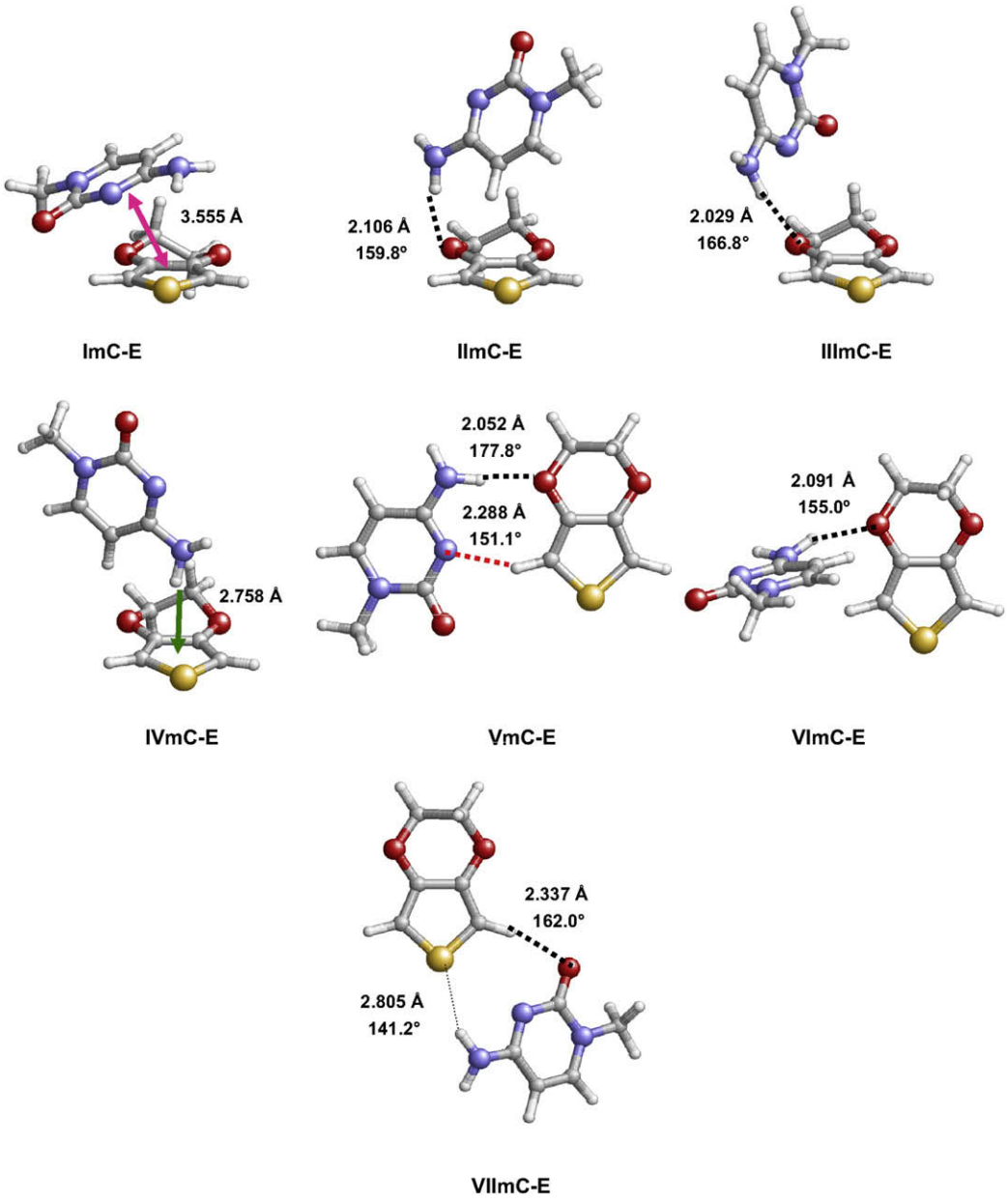

Fig. 8. Geometries of the seven EDOT⋯mC minimum energy complexes calculated at the MP2/6-31G(d) level. N–H⋯O, C–H⋯N, N–H⋯π and π-stacking interactions are indicated by black dashed lines, pink dashed lines, green arrows and pink arrows, respectively. Hydrogen bonding parameters (distances and angles) are displayed. (For interpretation of the references to color in this figure legend, the reader is referred to the web version of this article.)

units of the 11 Th⋯mNA minimum energy complexes previously characterized [18] were transformed into EDOT units; and (ii) 15 EDOT⋯mNA hydrogen bonded complexes were constructed using the oxygen atoms of the dioxane ring as interaction sites. Geometry optimization and frequency calculations at the MP2/6-31G(d) level provided the following distribution of minimum energy complexes: 6 EDOT⋯mA, 3 EDOT⋯mT, 7 EDOT⋯mC and 9 EDOT⋯mG, which are displayed in Figs. 6–9, respectively. Single point calculations at the MP2/6-311++G(d,p) level allowed to obtain accurate estimation of the both the relative stabilities and the affinities. Table 1 lists the relative energies ($\Delta E_{r,g}$), the relative free energies ($\Delta G_{r,g}$), and the binding energies, which were estimated with and without correct the basis set superposition error ($\Delta E^{CP}_{b,g}$ and $\Delta E_{b,g}$ respectively), for all the minimum energy complexes.

The EDOT⋯mA minimum of lowest energy (ImA–E) is stabilized by a strong hydrogen bond between the amino group of mA and one of the oxygen atoms of the dioxane ring. The remaining minima, which show $\Delta G_{r,g} \leq 2$ kcal/mol, present N–H⋯O (IImA–E), N–H⋯π (IIImA–E and IVmA–E) or both N–H⋯O and C–H⋯N interactions (VmA–E and VImA–E). However, the most striking feature is that $\Delta E^{CP}_{b,g}$ values range from −6.9 kcal/mol (ImA–E) to −4.7 kcal/mol (IIImA–E). These results differ significantly from those obtained for the Th⋯mA and Py⋯mA minimum energy complexes previously reported [18]. Thus, the $\Delta E^{CP}_{b,g}$ values calculated for the three Th⋯mA minima, which were stabilized by N–H⋯π interactions, were comprised between −4.5 and −3.7 kcal/mol, while those of the four N–H⋯N hydrogen bonded complexes found for Py⋯mA ranged from −9.3 to −8.3 kcal/mol. These results reflect than the affinity of EDOT by mA is higher than that of Th, even though it is lower than that of Py.

A completely different situation appears when the building block of PEDOT interacts with mT. In this case three minimum

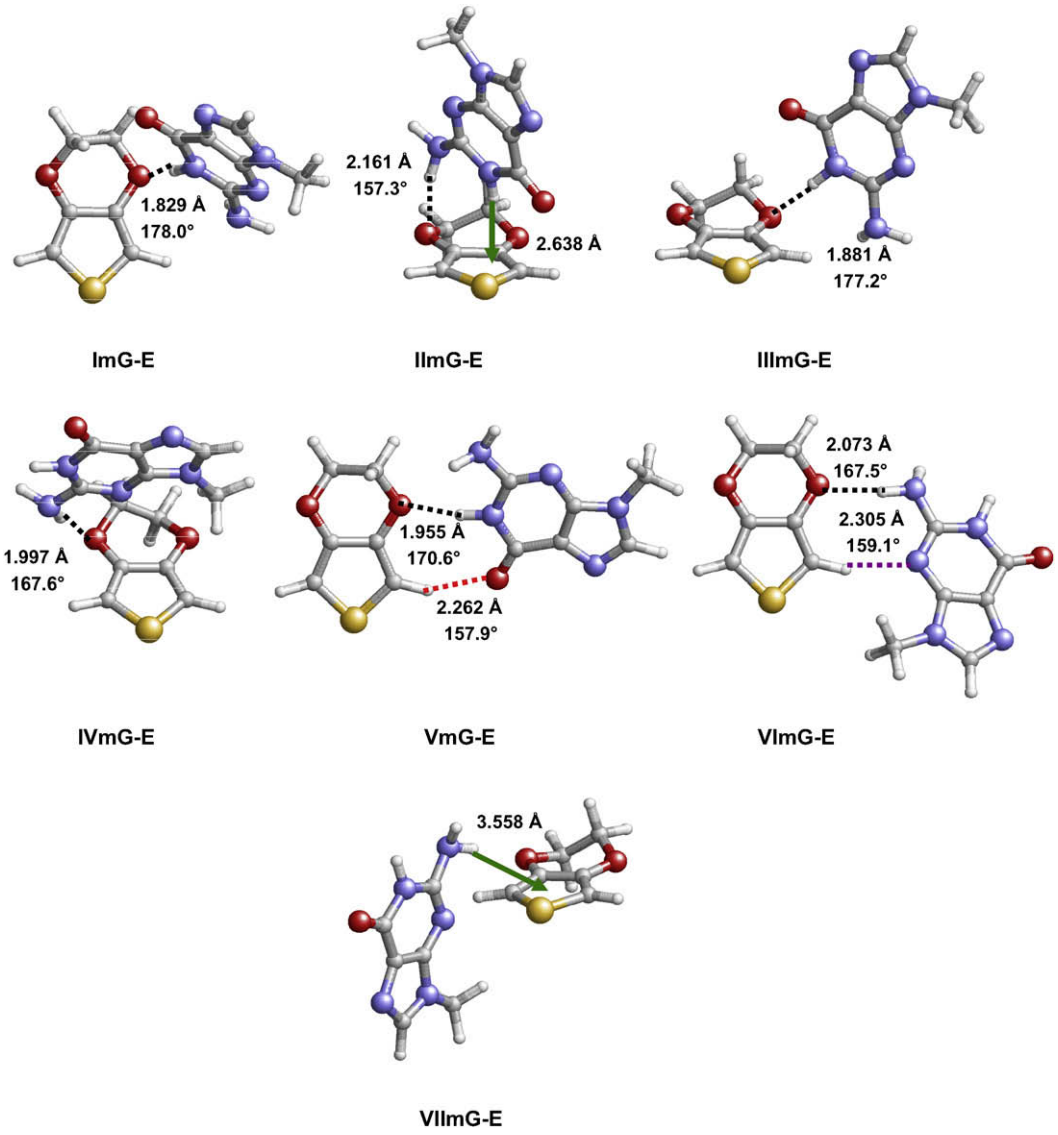

Fig. 9. Geometries of the seven EDOT⋯⋯mG minimum energy complexes calculated at the MP2/6-31G(d) level. N–H⋯O, C–H⋯O, C–H⋯N and N–H⋯π interactions are indicated by black dashed lines, red dashed lines, purple dashed lines and green arrows, respectively. Hydrogen bonding parameters (distances and angles) are displayed. (For interpretation of the references to color in this figure legend, the reader is referred to the web version of this article.)

energy complexes, which are almost isoenergetic ($\Delta G_{r,g} \leq 0.5$ kcal/mol), have been characterized. The most stable one (ImT–E) presents an N–H⋯π interaction, while the other two (IImT–E and IIImT–E) show N–H⋯O hydrogen bonds. Five minimum energy complexes with $\Delta G_{r,g} \leq 0.7$ kcal/mol were found for Py⋯mT: the lowest energy one showed a π-stacked arrangement and the other four were stabilized by N–H⋯O hydrogen bonds.[6] In contrast, a single minimum forming an N–H⋯π interaction was detected for Th⋯mT [18]. Interestingly, our calculations indicate that the strength of the interaction with mT is significantly higher for EDOT than for Py and Th. Thus, $\Delta E^{CP}_{b,g}$ is −10.3 kcal/mol for ImT–E and about −8 kcal/mol for IImT–E and IIImT–E, whereas it ranges from −7.7 to −6.6 in Py⋯mT complexes and is −3.8 kcal/mol for the Th⋯mT complex.

Inspection of the results obtained for EDOT⋯mC complexes suggests that the affinity of EDOT towards mC is similar to that obtained for Py. However, a detailed analysis of the structures evidences that the behavior of the two building blocks is completely different. Thus, 7 minimum energy complexes have been found for EDOT⋯mC, even though only 3 of them show $\Delta G_{r,g} \leq 2$ kcal/mol. The $\Delta E^{CP}_{b,g}$ values predicted for the latter structures, which are stabilized by π-stacking (ImC–E) and N–H⋯O hydrogen bonds (IImC–E and IIImC–E), are −9.1, −6.7 and −6.1 kcal/mol, evidencing that the strength of the former interaction is higher than that of the latter. In contrast, the three complexes characterized for Py⋯mC, which were close in energies ($\Delta G_{r,g} \leq 1.0$ kcal/mol), were stabilized by N–H⋯O and N–H⋯N hydrogen bonds, and the calculated $\Delta E^{CP}_{b,g}$ values ranged from −9.7 to −8.4 kcal/mol [18]. Accordingly, hydrogen bonds with mC are stronger for Py than for EDOT, even although the latter tends to form very stable π-stacking interactions with this mNA. Regarding to Th⋯mC, the $\Delta E^{CP}_{b,g}$ obtained for the three minimum energy complexes were ∼−4.5 kcal/mol [18], which indicate that Th provides the weakest interaction.

On the other hand, seven minimum energy complexes were obtained for EDOT⋯mG, five of them showing $\Delta G_{r,g} < 2$ kcal/mol. The $\Delta E^{CP}_{b,g}$ of the lowest energy one (ImG–E), which is stabilized by an N–H⋯O hydrogen bond, is −9.8 kcal/mol. The $\Delta E^{CP}_{b,g}$ of the second complex (IImG–E) is higher by 0.6 kcal/mol, even though it involves both an N–H⋯O hydrogen bond and an N–H⋯π

Table 1
Relative free energy[a] and energy[b] in the gas-phase ($\Delta G_{r,g}$ and $\Delta E_{r,g}$; in kcal/mol), and binding energies[c] with and without correct the basis set superposition error ($\Delta E^{CP}_{b,g}$ and $\Delta E_{b,g}$; in kcal/mol) for EDOT···mNA complexes.

	$\Delta G_{r,g}$	$\Delta E_{r,g}$	$\Delta E^{CP}_{b,g}$	$\Delta E_{b,g}$
EDOT···mA				
ImA–E	0.0	0.5	−6.9	−16.2
IImA–E	0.4	0.0	−6.7	−10.4
IIImA–E	0.9	2.1	−4.7	−8.1
IVmA–E	1.5	2.3	−5.6	−8.2
VmA–E	1.7	1.8	−5.6	−8.7
VImA	2.0	2.4	−5.5	−8.1
EDOT···mT				
ImT–E	0.0	0.8	−10.3	−5.4
IImT–E	0.3	0.0	−7.9	−11.5
IIImT–E	0.5	0.0	−8.0	−11.5
EDOT···mC				
ImC–E	0.0	3.2	−6.0	−13.8
IImC–E	1.6	1.7	−6.7	−11.8
IIImC–E	1.7	1.0	−9.1	−12.8
IVmC–E	3.0	3.2	−5.8	−10.3
VmC–E	4.3	4.3	−6.5	−9.4
VImC–E	4.5	4.4	−5.8	−9.1
VIImC–E	5.9	5.9	−4.6	−7.6
EDOT···mG				
ImG–E	0.0	0.0	−9.8	−14.4
IImG–E	0.4	0.6	−9.2	−13.9
IIImG–E	1.0	0.5	−7.4	−13.3
IVmG–E	1.3	0.9	−8.6	−13.1
VmG–E	1.3	0.5	−7.0	−13.3
VImG–E	2.7	3.1	−7.5	−11.0
VIImG–E	3.3	4.6	−5.9	−9.2
VIIImG–E	4.5	5.5	−4.4	−8.0

[a] Estimated by adding the thermodynamic corrections obtained at the MP2/6-31G(d) level to the electronic energies calculated at the MP2/6-311++G(d,p) level using the MP2/6-31G(d) geometries.
[b] Derived from single point calculations at the MP2/6-311++G(d,p) level on MP2/6-31G(d) geometries.
[c] Binding energies were calculated at the MP2/6-311++G(d,p) level.

Table 2
Free energies of solvation (ΔG^{CHL}_{sol} and ΔG^{WAT}_{sol}; in kcal/mol), relative free energies[a] ($\Delta G_{r,CHL}$ and $\Delta G_{r,WAT}$; in kcal/mol) and binding energies[b] ($\Delta E^{CP}_{b,CHL}$ and $\Delta E^{CP}_{b,WAT}$; in kcal/mol) in the chloroform (CHL) and aqueous (WAT) solutions for EDOT···mNA complexes.

	ΔG^{CHL}_{sol}	ΔG^{WAT}_{sol}	$\Delta G_{r,CHL}$	$\Delta G_{r,WAT}$	$\Delta E^{CP}_{b,CHL}$	$\Delta E^{CP}_{b,WAT}$
EDOT···mA						
ImA–E	−3.5	−4.0	0.1	0.3	−0.9	0.9
IImA–E	−4.0	−4.8	0.0	0.0	−1.1	0.5
IIImA–E	−4.3	−5.1	0.2	0.2	0.7	1.8
IVmA–E	−4.0	−4.9	1.0	0.9	−0.1	1.3
VmA–E	−3.8	−4.7	1.4	1.3	0.0	1.5
VImA–E	−3.9	−4.8	1.6	1.5	−0.1	1.3
EDOT···mT						
ImT–E	−1.8	−2.7	0.0	0.0	−2.2	−0.3
IImT–E	−1.9	−2.1	0.3	1.0	0.2	2.9
IIImT–E	−1.7	−1.7	0.6	1.5	0.3	3.2
EDOT···mC						
ImC–E	−11.5	−17.8	0.0	0.0	−2.1	−2.3
IImC–E	−9.6	−13.5	3.4	5.8	−0.8	1.5
IIImC–E	−6.4	−9.2	6.8	10.3	0.5	4.3
IVmC–E	−7.0	−11.1	4.4	6.6	−0.6	1.4
VmC–E	−9.1	−14.1	8.3	9.6	1.9	3.3
VImC–E	−8.2	−12.8	7.6	9.2	0.7	2.3
VIImC–E	−10.0	−14.3	6.0	7.9	−0.4	1.5
EDOT···mG						
ImG–E	−10.6	−15.9	2.6	4.1	−6.7	1.1
IImG–E	−8.9	−13.7	4.6	6.6	2.2	5.6
IIImG–E	−10.0	−14.5	4.2	6.4	2.3	5.1
IVmG–E	−10.0	−14.9	4.5	6.3	0.8	3.8
VmG–E	−14.6	−21.3	0.0	0.0	−2.6	−1.6
VImG–E	−10.6	−15.9	5.3	6.7	−4.4	3.5
VIImG–E	−13.8	−19.3	3.2	3.9	−0.3	1.3
VIIImG–E	−13.3	−20.1	4.0	4.3	0.6	2.0

[a] Estimated by adding the free energies of salvation to the $\Delta G_{r,g}$ values (Table 1).
[b] Estimated considering the $\Delta E^{CP}_{b,g}$ values (Table 1) and the free energies of solvation calculated for the dimers and the corresponding monomers.

interaction. The next two minima, IIImG–E and IVmG–E, are stabilized by N–H···O hydrogen bonds, and show $\Delta E^{CP}_{b,g}$ values of −7.4 and −8.6 kcal/mol, respectively. Finally, the strength of the binding produced by the N–H···O and C–H···O interactions found in VmG–E is −7.0 kcal/mol. These results differ significantly from those obtained for the four complexes obtained for Th···mG,[6] which showed $\Delta E^{CP}_{b,g}$ values ranging between −6.8 and −4.0 kcal/mol. All these structures were stabilized by N–H···π interactions rather than by intermolecular hydrogen bonds. The five minimum energy complexes calculated for Py···mG are predominantly stabilized by hydrogen bonds, even although $\Delta G_{r,g} \geq 2.8$ kcal/mol for four of them.[6] The $\Delta E^{CP}_{b,g}$ of the lowest energy one was −12.5 kcal/mol, while the strength of the interaction ranged from −8.7 to −7.5 kcal/mol for the other minima.

The free energies of solvation for EDOT···mNA complexes were calculated using a Self-Consistent Reaction-Field (SCRF) method. Table 2 includes the relative free energy ($\Delta G_{r,CHL}$ and $\Delta G_{r,WAT}$) and binding energy ($\Delta E^{CP}_{b,g}$ and $\Delta E^{CP}_{b,WAT}$) calculated for EDOT···mNA complexes in both chloroform (CHL) and aqueous (WAT) solutions. As can be seen, the solvent produces some changes into the relative stabilities of both EDOT···mT and EDOT···mC complexes, even though they are not significant. Specifically, the lowest energy complex in the two solvents is the same that in the gas-phase, *i.e.* ImT–E and ImC–E, respectively, whereas the contribution of the other low-energy structures vary with the polarity of the environment. On the other hand, the effect of the solvent on the stability of the six EDOT···mA minimum energy structures is small. Thus, independently of the environment all the structures are within a free energy interval smaller than 2 kcal/mol. In contrast, the influence of the solvent on the relative stabilities of the EDOT···mG complexes is very remarkable. Thus, in this case VmG–E, which was destabilized by 1.3 kcal/mol in the gas-phase, was found to be the lowest free energy structure in both chloroform and aqueous solution. Moreover, the contribution of all the other structures was negligible, *i.e.* $\Delta G_{r,CHL} \geq 2.6$ kcal/mol and $\Delta G_{r,WAT} \geq 3.9$ kcal/mol, even although they showed $\Delta G_{r,g} < 2.0$ kcal/mol.

Analysis of the influence of the solvent on the strength of the binding reveals very remarkable features. Specifically, the interaction between mNA and EDOT has been predicted to be attractive in many cases. In chloroform solution the values of $\Delta E^{CP}_{b,CHL}$ obtained for IImA–E, ImT–E, ImC–E and VmG–E, which are the complexes with lowest $\Delta G_{r,CHL}$, are −1.1, −2.2, −2.1 and −2.6 kcal/mol, respectively. On the other hand, ImT–E, ImC–E and VmG–E are the only complexes with an attractive binding in aqueous solution, *i.e.* $\Delta E^{CP}_{b,WAT}$ is −0.3, −2.3 and −1.6 kcal/mol, respectively. It should be mentioned that repulsive interactions were predicted in aqueous solution for all the Py···mNA and Th···mNA complexes [18]. Thus, the strength of the binding with mNA undergoes a solvent-induced reduction that is more drastic for Py and Th than for EDOT. Although the local polarity in the interaction sites is not known, it is probably smaller and larger than that of water and chloroform, respectively. Therefore, the results derived from MP2 calculations on model complexes are fully consistent with experimental data.

4. Conclusions

This work presents a detailed study about the interaction of plasmid DNA with PEDOT, a conducting polymer with excellent electrical, electrochemical and environmental properties. Ultrafine particles of PEDOT were obtained by applying ultrasounds to the grinded samples of polymer, which was prepared by anodic electropolymerization. Electrophoresis, UV–visible and CD results obtained for mixtures of pMT4 plasmid DNA and PEDOT with

different mass ratios indicate that interactions form immediately giving place to stable adducts. Moreover, electrophoretograms obtained after digestion with restriction enzymes show that the conducting polymer interact with specific nucleotide sequences, *i.e.* 5′-G/AATTC-3′ (target for EcoRI) and 5′-G/GATCC-3′ (target for BamHI). Completely different results have been obtained for PT3M, a polythiophene derivative without donor and acceptors of hydrogen bonds. Thus, depending on the mass ratios, interactions between the latter material and plasmid DNA have been not detected or have been found to be weak. These features suggest that hydrogen bonds are essential to determine the specificity for selected nucleotide sequences and to define the strength and temporal evolution of the interactions between the conducting polymer and the plasmid DNA.

On the other hand, the CD spectra clearly show that the interaction with conducting polymers provokes an alteration in the secondary structure of DNA, *i.e.* the unfolding of the double helix, which increases the exposition of the nitrogen bases. Both this result and the importance of hydrogen bonds in specific interactions lead us to propose the following hypothesis for the interaction between DNA and conducting polymers: the latter materials produce the unfolding of the double helix promoting its intercalation between the DNA strands. This enhances the exposition of the DNA bases and, in the case of PEDOT, allows the formation of hydrogen bonding interactions between the bases and the oxygen atoms of the dioxane ring. The absence of these specific interactions explains the higher degree of exposition found in DNA:PT3M mixtures.

Ab initio quantum mechanical calculations in different environments show that the interactions with nucleic acid basis are stronger for EDOT than for Thp. Indeed, EDOT usually interact through specific hydrogen bonds, while Th only forms complexes stabilized by interactions between the π-cloud of the ring and N–H groups of nucleic acid bases. These features are fully consistent with the experimental results presented for PEDOT and PT3M. On the other hand, the affinity towards the DNA bases are completely different for EDOT and Py, which should be attributed to the chemical characteristics of the oxygen atoms of EDOT (hydrogen bonding acceptors) and the N–H group of Py (hydrogen bonding donor). The strength of the binding in the gas-phase for EDOT$\cdots$mNA complexes grows in the following order: $mA < mC < mG \approx mT$. Furthermore, EDOT retains a significant affinity towards DNA bases when the polarity of the environment increases, whereas repulsive interactions were predicted for Py$\cdots$mNA complexes in a polar solvent.

The overall results presented in this work indicate that PEDOT, which was found to be a biocompatible material [22,23], is a potential candidate for the development electroactive devices, *e.g.* drug-delivery systems, able to act through specific molecular recognition patterns.

Acknowledgements

This work has been supported by MCYT and FEDER with Grant MAT2006-04029. Authors are indebted to the Centre de Supercomputació de Catalunya (CESCA) for computational facilities.

References

[1] Chriswanto H, Wallace GG. J Liq Chromatogr 1996;19:2457.
[2] Miller LL, Zinger B, Zhou OX. J Am Chem Soc 1987;109:2267.
[3] Guo H, Knobler CM, Kaner RB. Synth Met 1999;101:44.
[4] Englebienne P. J Mater Chem 1999;9:1043.
[5] Kros A, van Howell SWFM, Sommerdijk NASM, Nolte RJM. Adv Mater 2001;13:1555.
[6] Khan GF, Wernet W. Thin Solid Films 1997;300:265.
[7] Azioune A, Chehimi MM, Miksa B, Basinska T, Slomkowski S. Langmuir 2002;18:1150.
[8] Misoska V, Prize WE, Ralph S, Wallace GG. Synth Met 2001;123:279.
[9] Wang J, Jiang M. Electroanalysis 2001;13:537.
[10] Ho H-A, Boissinot M, Bergeron MG, Corbeil G, Dore K, Boudreau D, et al. Angew Chem Int Ed 2002;41:1548.
[11] Minehan DS, Marx KA, Tripathy SK. Macromolecules 1994;27:777.
[12] Bae A-H, Hatano T, Numata M, Takeuchi M, Shinkai S. Macromolecules 2005;38:1609.
[13] Peng H, Zhang L, Spires J, Soeller C, Travas-Sejdic J. Polymer 2007; 48:3413.
[14] Yamamoto T, Shimizu T, Kurokawa E. React Funct Polym 2000;43:79.
[15] Ocampo C, Armelin E, Estrany F, del Valle LJ, Oliver R, Sepulcre F, et al. Macromol Mater Eng 2007;292:85.
[16] Teixeira-Dias B, del Valle LJ, Estrany F, Armelin E, Oliver R, Alemán C. Eur Polym J 2008;44:3700.
[17] Pfeiffer P, Armelin E, Estrany F, del Valle LJ, Cho LY, Alemán C. J Polym Res 2008;15:225.
[18] Zanuy D, Alemán C. J Phys Chem B 2008;112:3222.
[19] Liu B, Bazán GC. Chem Mater 2004;16:4467.
[20] Schmidt CE, Shastri V, Vacanti JP, Langer R. Proc Natl Acad Sci U S A 1997;94:8948.
[21] Kotwal A, Schmidt CE. Biomaterials 2001;22:1055.
[22] del Valle LJ, Aradilla D, Oliver R, Sepulcre F, Gamez A, Armelin E, et al. Eur Polym J 2007;43:2342.
[23] del Valle LJ, Estrany F, Armelin E, Oliver R, Alemán C. Macromol Biosci 2008;8:1144.
[24] Wallace GG, Kane-Maguire LAP. Adv Mater 2002;14:953.
[25] Adhikari B, Majumdar S. Prog Polym Sci 2004;29:699.
[26] Ocampo C, Oliver R, Armelin E, Alemán C, Estrany F. J Polym Res 2006;13:193.
[27] Goenendaal LB, Jonas F, Freitag D, Pielartzik H, Reynolds JR. Adv Mater 2000;12:481.
[28] Pei Q, Zuccarello G, Ahlskog M, Inganäs O. Polymer 1994;35:1347.
[29] Estrany F, Aradilla D, Oliver R, Alemán C. Eur Polym J 2007;43:1876.
[30] Frisch MJ, Trucks GW, Schlegel HB, Scuseria GE, Robb MA, Cheeseman JR, et al. Gaussian 03, Revision B.02. Pittsburgh, PA: Gaussian, Inc.; 2003.
[31] Møller C, Plesset M. Phys Rev 1934;46:618.
[32] Hariharan PC, Pople JA. Theor Chim Acta 1972;28:203.
[33] Frisch MJ, Pople JA, Binkley JS. J Chem Phys 1984;80:3265.
[34] Boys SF, Bernardi F. Mol Phys 1970;19:553.
[35] Miertus M, Scrocco E, Tomasi J. Chem Phys 1981;55:117.
[36] Miertus S, Tomasi J. Chem Phys 1982;65:239.
[37] Hawkins GD, Cramer CJ, Truhlar DG. J Chem Phys B 1998;102:3257.
[38] Jang YH, Goddard III WA, Noyes KT, Sowers LC, Hwang S, Chung DS. J Phys Chem B 2003;107:344.
[39] Iribarren JI, Casanovas J, Zanuy D, Alemán C. Chem Phys 2004;302:77.
[40] Nejedly K, Chládková J, Vorlícková M, Hrabcová I, Kypr J. Nucleic Acids Res 2005;33:e5.
[41] Braun CS, Jas GS, Choosakoonkriang S, Koe GS, Smith JG, Middaugh CR. Biophys J 2003;84:1114.
[42] Casanovas J, Alemán C. J Phys Chem C 2007;111:4823.
[43] Brédas JL. J Chem Phys 1985;82:3808.
[44] Hernandez V, Castiglioni C, Del Zopo M, Zerbi G. Phys Rev B 1994;50:9815.
[45] Zade SS, Bendikov M. J Phys Chem C 2007;111:10662.
[46] Zade SS, Bendikov M. J Phys Chem B 2006;110:15839.